

Evaluation of Concrete Consolidation: DSS-35 Antenna Reinforced Concrete Pedestal Canberra Deep Space Communications Complex, Australia

Benjamin P. Saldua,* Ethan C. Dodge,† Peter R. Kolf,† and Carlton A. Olson†

ABSTRACT. — Antenna structures for the Deep Space Network track spacecraft that are millions of miles away. Therefore, these structures have tight specifications for translation, rotation, and differential settlement. This article presents several nondestructive test methods that were used to evaluate, locate, and repair imperfections in the reinforced concrete pedestal that supports the DSS-35 antenna structure. These methods include: (1) impulse response (IR), (2) ultrasonic shear-wave tomography (MIRA), and (3) ground-penetrating radar (GPR).

I. Introduction

The Deep Space Network (DSN) is a National Aeronautics and Space Administration (NASA) entity. It is managed, technically directed, and operated by the Jet Propulsion Laboratory (JPL) of the California Institute of Technology (Caltech). The objectives of the DSN are to maintain communications with spacecraft. This consists of collecting telemetry data from the spacecraft, transmitting command data to them, providing spacecraft trajectory data to mission operations and scientists, and monitoring and controlling the network performance. Other objectives are to gather science data from spacecraft, to measure variations in transmitted radio waves from spacecraft for radio science experiments, and to perform very long baseline interferometry observations. The DSN is the largest and most sensitive scientific telecommunications and radio navigation network in the world.

The DSN consists of three deep-space communications complexes (DSCCs) separated by approximately 120 deg of longitude around the world. These complexes are at Goldstone, near Barstow, California; near Madrid, Spain; and near Canberra, Australia. The strategic placement of these sites permits constant communication with spacecraft as our planet rotates — before a distant spacecraft sinks below the horizon at one DSN site, another site can pick up the signal and continue communicating.

NASA/JPL is currently replacing the large 70-m antennas at each complex with arrays of 34-m-diameter antennas. The 34-m beam-waveguide (BWG) antennas are dual-shaped Cassegrain reflector antennas. They are characterized by an elevation over azimuth design, where the elevation tipping structure is supported by an alidade structure that has a wheel-

* Communications Ground Systems Section.

† CTLGroup, Skokie, Illinois.

The research described in this publication was carried out by the Jet Propulsion Laboratory, California Institute of Technology, under a contract with the National Aeronautics and Space Administration. © 2016. All rights reserved.

and-track azimuth bearing system that provides rotation about the vertical axis (Figure 1). The alidade corners are supported on wheeled carriage (truck) assemblies that roll on a precisely aligned steel track resting on a massive circular concrete foundation. The wheel-and-track assembly is stabilized laterally by a pintle bearing at the top of a concrete wall cast integrally with the pedestal roof slab. The pintle bearing area contains a cable wrap-up device to accommodate the motions of the many electrical and microwave cable conduits during azimuth rotation. The pedestal, typically constructed of reinforced concrete, is high enough to allow the antenna rim to clear the ground when the antenna tips to low elevation positions. The roof of the pedestal measures 64 ft in diameter and is 2 ft thick.

DSS-35 is the latest addition of 34-m BWG-class antennas to the DSN. It is located in the Canberra Deep Space Communications Complex (CDSCC) in Australia (Figure 1), and it entered into service in October 2014. At the time of pedestal construction, during an inspection conducted in January 2012, it was observed that the DSS-35 antenna outer track surface and slab soffit suffered from poor concrete consolidation. These deficiencies raised the concern that internal voiding in the concrete might be present.

The general contractor who performed the original pedestal work contracted with several local testing firms to identify concrete consolidation deficiencies. They deployed ground-penetrating radar (GPR) and ultrasonic pulse velocity (UPV) test methods. In addition, they removed and tested concrete cores but found no correlation between test method findings and core conditions. Given the lack of satisfactory results by the contractor, JPL decided to conduct its own investigation utilizing alternate nondestructive test methods by its specialized in-house engineering team.

The scope of the project work included evaluation of concrete consolidation, development of a conceptual design for its repair, and site repair observations for the reinforced concrete antenna pedestal structure. An overall view of DSS-35 is shown in Figure 1. Overall, it was determined that a combination of hot weather, equipment breakdown, low slump concrete mix, and poor workmanship resulted in these concrete consolidation deficiencies.



Figure 1. 34-m antenna assembled on support structure.

The application of nondestructive testing to identify areas with concrete deficiencies and a statistically based analysis method for interpretation of the data are presented. A repair procedure based on nondestructive test results, type of concrete deficiency and requirements of the structure is also presented.

II. Structure and Problem

The structure is a circular reinforced concrete antenna pedestal with one level below grade and a roof slab at approximately grade elevation. The structure contains an outer track wall with an inner radius of 9365 mm (30.7 ft), a width of 900 mm (35.4 in.), and a height of approximately 360 mm (14.2 in.) above the roof slab. The pintle wall at the center of the roof structure has an inner diameter of 2743 mm (9 ft), a width of 600 mm (23.6 in.), and a height of 790 mm (31.1 in.). The roof slab of the structure is 600 mm thick at the perimeter track and thickens toward the pintle in order to provide a 1 percent drainage slope. The roof slab is reinforced with radial and circumferential reinforcing.

Concrete placement of the roof slab and outer track wall began by filling the outer track forms and adjacent main roof slab to approximately the roof slab final elevation and then continued from the center outward in wedge shaped sections (Figure 2). After the outer track had stiffened enough to be filled above the main slab elevation, the final layer was placed and the lifts vibrated together. Experience has shown that the most likely problem areas would be the lift line between outer perimeter lifts and below the lap splices of the upper and lower reinforcing mats in the roof slab. Poor concrete consolidation was visible at the roof slab underside below the lower mat lap splices at the time of form removal. These locations had been chipped to sound concrete at the time that the investigation commenced (Figure 3).



Figure 2. Concrete placement.

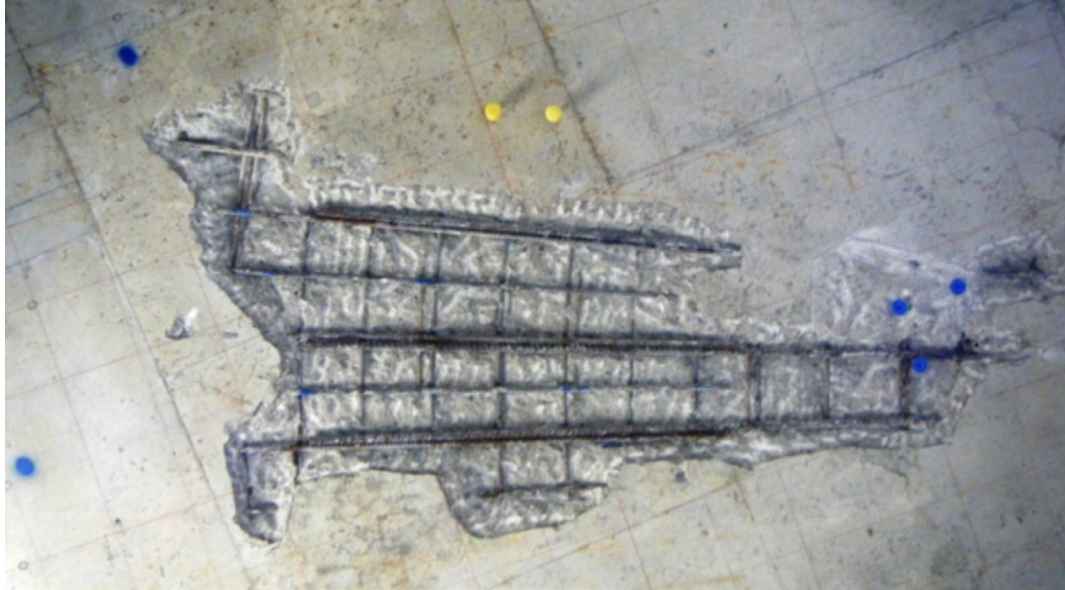


Figure 3. Concrete removal identified bar laps at a location of voiding at the slab soffit.

III. Test Program

An orthogonal grid spacing of 300 mm in each of four quadrants was used on the topside and underside of the roof slab (Figure 4). Some locations with underside chipping were superimposed onto the top surface using blue paint. Approximately 7000 impulse response (IR) (ASTM C1740-10) tests were conducted on the top surface and the majority of the soffit.

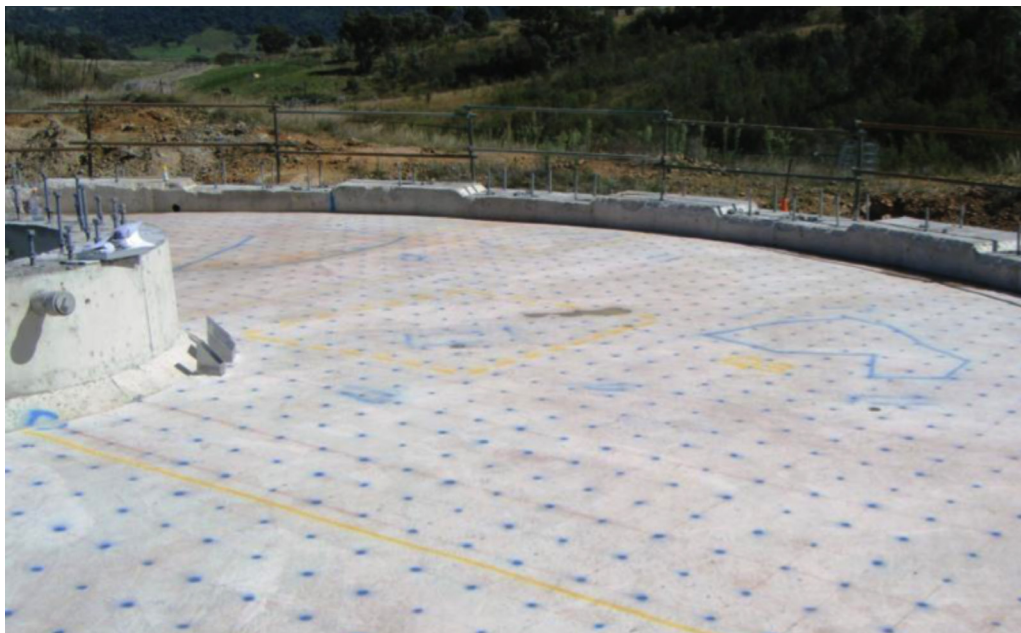


Figure 4. Test grid marked on slab topside (blue lines outline underside concrete removal areas).

The IR test method utilizes a low-strain impact from a 1-kg hammer with a built-in load cell to excite the structure. The maximum compressive stress at the impact point in concrete is directly related to the elastic properties of the hammer tip. The response to the impact stress is normally measured by a velocity transducer (geophone). The geophone velocity spectrum is divided by the force spectrum to obtain a transfer function, referred to as the mobility of the element under test.

Locations were selected for the application of ultrasonic shear-wave tomography (UST) testing technique (commonly known as “MIRA”) based on the IR test results and visual observations. MIRA is a phased-array system applicable for nondestructive concrete testing using low-frequency ultrasonic wave (20 to 100 kHz) and advanced methods of signal processing. This system represents one of the most advanced techniques currently available in diagnosing defects in concrete, especially large concrete structures. This equipment is used to image the internal condition of a concrete structure using a pulse-echo technique, conducted from one side of the test element. Presence of internal defects such as cracks, voids, etc., and their approximate depths and extents can be evaluated.

Contour maps displaying the average mobility values were generated from the IR data. These maps, combined with MIRA test results, visual observations, and hammer sounding, were used to select areas for concrete coring and investigative concrete removal.

Ground-penetrating radar (GPR) was utilized to lay out the location of reinforcing steel prior to coring. GPR uses high-frequency electromagnetic energy, typically 900 to 2600 MHz, for rapidly and continuously assessing a variety of characteristics of the subsurface being tested. A single contacting transducer (antenna) is used for transmitting and receiving radar signals. High-frequency, short-pulse electromagnetic energy is transmitted into the tested medium (usually concrete or soil). Each transmitted pulse travels through the element being tested, and is partially reflected when it encounters a change in dielectric constant such as a change in material type, a void, reinforcing steel, etc.

Because IR is a relative test method that measures the response of a structure to a known force input, measured changes in structural response are evaluated by performing statistical analyses, performing additional testing such as I-E (impact echo) testing or MIRA and by destructively opening areas and/or removing core samples for visual inspection. A total of 17 concrete cores were removed to confirm the IR test results and to support the visual observations. IR average mobility test results for the top surface combined with core locations that are color-coded for observed conditions are shown in Figure 5. The four quadrants have been combined to show the test results for the entire roof slab. A close-up of Quadrant 2 is shown in Figure 6.

IV. IR Data Analysis

For the data analysis, the roof slab was divided into four separate designated quadrants (Quadrants 1 through 4). Given that the computed IR average mobility values from each quadrant were statistically similar, it was decided to perform the analysis on the ensemble

of the combined dataset. The basic assumption used to interpret the IR data is that portions of the structure do not contain defects or changes in structural condition. It is the sound uniform portion of the structure that is used to establish the expected structural response and appropriate standard deviations. Experience has shown that, typically, sufficient sound areas are present to perform this analysis even when significant defective regions are also present. Application of the statistical analysis method to average mobility values identifies the following general guidelines for comparison with the expected structural response:

- (1) Average mobility values within 2 standard deviations of the mean are as expected, and do not indicate significant changes in concrete condition.
- (2) Average mobility values between 2 and 4 standard deviations of the mean are indicative of material changes. These include lower strength, increased entrapped air voids, surface deterioration, or other minor localized defects.
- (3) Average mobility values greater than 4 standard deviations from the mean indicate significant concrete deficiencies.

The expected structural response (average of all areas without significant defects) used was an IR mobility value of 0.275 with a standard deviation of 0.05. These values were obtained from Quadrant 4, which has very few defects, and are roughly consistent with values from the overall data after high values were removed (i.e., data with mobility values less than 0.425 or approximately 3 standard deviations from the mean). Approximately 95 percent of the values were within 2 standard deviations, 4 percent between 2 and 4 standard deviations and 1 percent greater than 4 standard deviations from the mean. The IR results showed widespread low-magnitude variation without visible signs of surface deterioration, indicating that subtle defects and material variations were probable.

Analysis of the values from each quadrant, all quadrants combined, and all values less than 0.425 is presented in Table 1.

Table 1. Average mobility results within 4 standard deviations of mean.

Name	Quadrant 4	Quadrant 3	Quadrant 2	Quadrant 1	All Data	Less Than 0.425
Average	0.280	0.268	0.278	0.284	0.278	0.273
Minimum	0.163	0.152	0.151	0.146	0.146	0.146
Maximum	0.541	0.783	1.512	0.689	1.512	0.423
Std Deviation	0.050	0.054	0.089	0.060	0.065	0.047
# Points	732	718	708	735	2756	2711

For this project, significant voids produced average mobility values greater than 0.475. The value of 0.475 corresponds to approximately 4 standard deviations from the average response which, in our experience, is commonly associated with significant defects in similar structures. All cores removed in or adjacent to areas with mobility greater than 0.475 revealed significant defects (Cores CTL-1, CTL-2, CTL-3, CTL-5, and CTL-9). All cores

removed in or adjacent to areas with mobility greater than 0.425 but less than 0.475 revealed signs of concrete irregularities (CTL-6, CTL-11, and Core 6). All cores removed in or adjacent to areas with mobility values within 2 standard deviations of the mean exhibited only minor irregularities.

V. MIRA Test Results

A significant void below the top reinforcing steel was distinguishable from the MIRA test results (Figure 7) at the location of Core CTL-2. However, in areas with material variations such as an increase in entrapped air pockets or the cold joint at the location of Core CTL-3, significant defects could not be distinguished by MIRA.

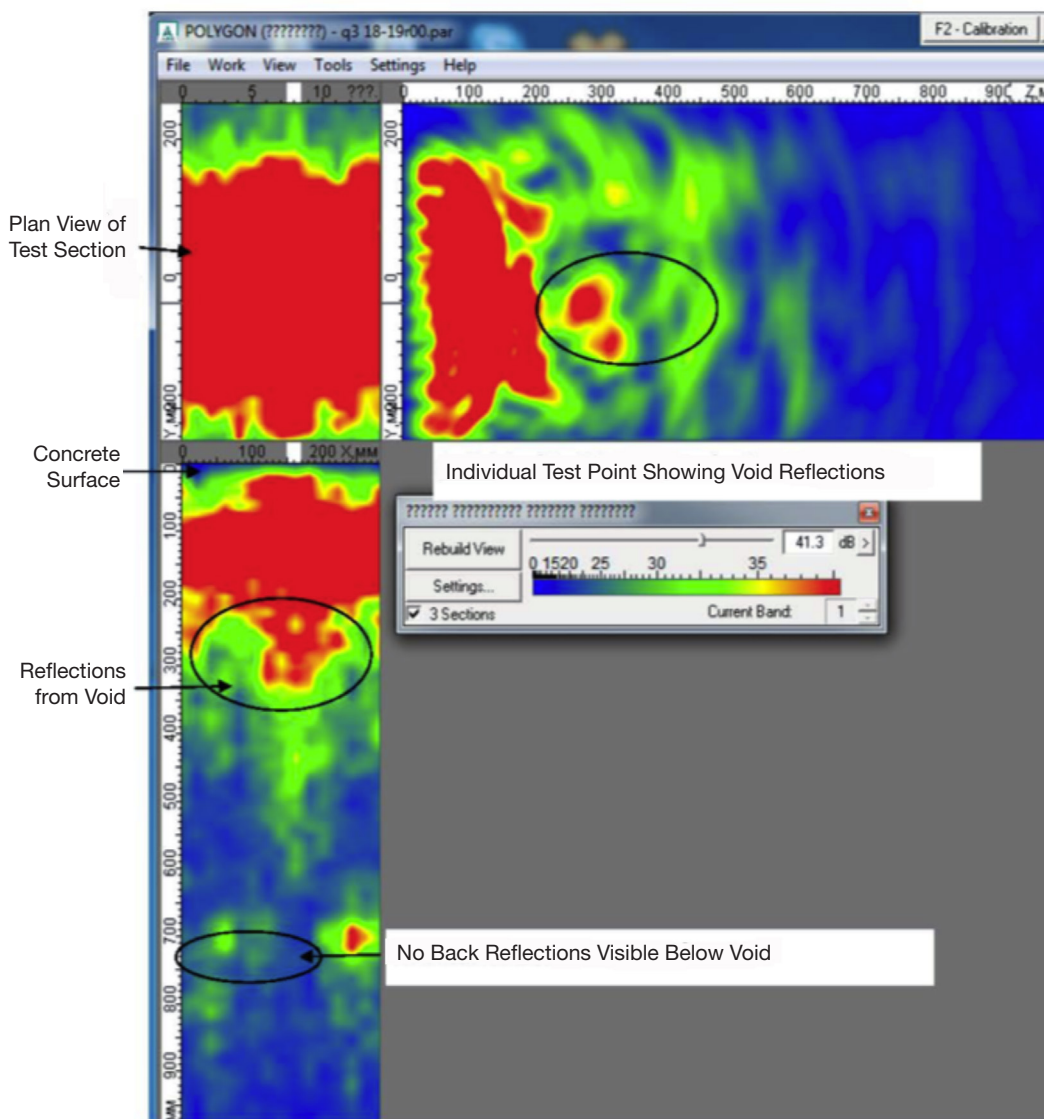


Figure 7. MIRA data showing a void below the upper reinforcing steel near the location of Core CTL-2.

VI. Repairs

Results of nondestructive testing and material sampling revealed that significant defects could be identified reliably and that the pedestal structure could be effectively repaired to restore structural integrity and long-term durability.

The repair program consisted generally of the following:

- (1) *Soffit* — As expected, and as demonstrated by the IR test results, significant defects on the slab underside were limited to primarily the lap spliced zones under the lower reinforcing mat. Shotcrete was selected as the repair material for the soffit repairs. Cavity areas above reinforcing steel were filled with trowel-grade mortar prior to shotcrete application. The preparation, cavity filling and final shotcrete repair are shown in Figure 8.

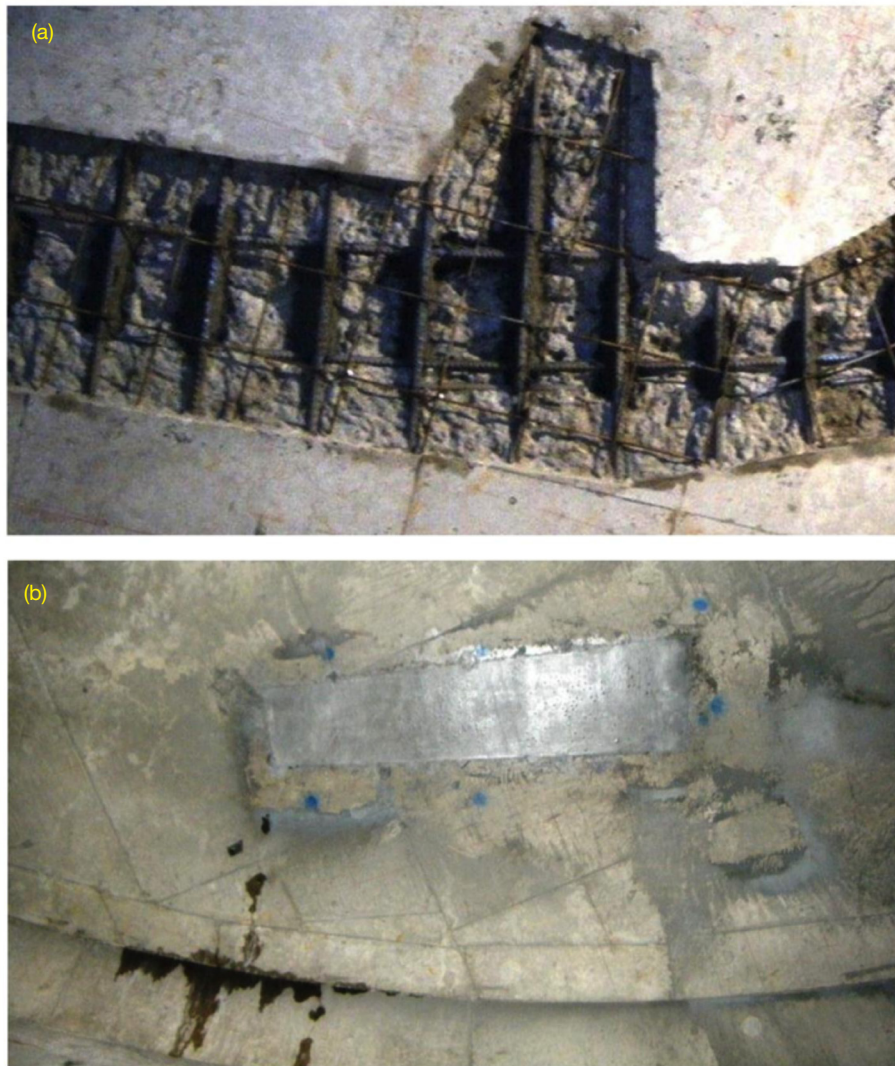


Figure 8. Soffit repair. (a) Soffit cavity prepared and mortar packed above reinforcing.
(b) Completed shotcrete repair.

- (2) *Perimeter track* — Presence of significant reinforcing in perimeter track walls precluded the use of nondestructive testing techniques. Therefore, a combination of visual inspection and careful exploratory concrete removal was used to identify areas of concrete for removal and replacement. Voids encountered were generally associated with areas of laps in reinforcing bars. Figure 9 shows repairs to an area of voiding at the track wall.
- (3) *Top surface* — The top surface repairs were primarily based off the IR test results as follows:
- A significant void or defect was presumed to exist at any location where the IR mobility test result was 0.475 or higher. Therefore, these locations were marked for concrete repairs. Repair excavations were expanded as necessary to remove any defective concrete.
 - Where adjacent IR test points indicated mobility values between 0.425 and 0.475, or single such IR points existed within regions with mobility values greater than 0.375 or adjacent to regions of known defects, coring was recommended to further define potential defects.
 - Where isolated IR test points with mobility values between 0.425 and 0.475 occurred adjacent to regions with mobility values less than 0.375, any potential defect was considered isolated and not in need of further investigation.
 - No significant defect was presumed to be present where mobility values were less than 0.425.

The core location (CTL-2), exploratory opening and the repair extents (in yellow) for a relatively large voided area can be seen in Figure 10. The repair of a voided area is shown in Figure 11. In addition to the repairs stemming from concrete placement delays, a poor bond between the wall placement and the roof slab placement was observed in localized areas. These areas were selected for epoxy injection repairs that are shown in Figure 12.

Acknowledgments

Many people were involved in the decisions and execution of this project. The authors would like to thank and acknowledge Tony Ross and David True (CDSCC), Asim Sehic (JPL), and David Drengenberg (CTLGroup) for their support on the nondestructive testing and actual repair. Special thanks to Neil Bucknam, John Cucchissi, Mark Gatti, Andre Jongeling, Hal Ahlstrom, and Peter Hames (JPL) for their managerial decisions and support.



Figure 9. Track wall repair. (a) Area of poor consolidation at track wall. (b) Poorly consolidated concrete removed and repair area prepared. (c) Completed placement of repair.



**Figure 10. Exploratory opening at location of Core CTL-2 encountered significant voiding.
The repair extents are shown in yellow.**

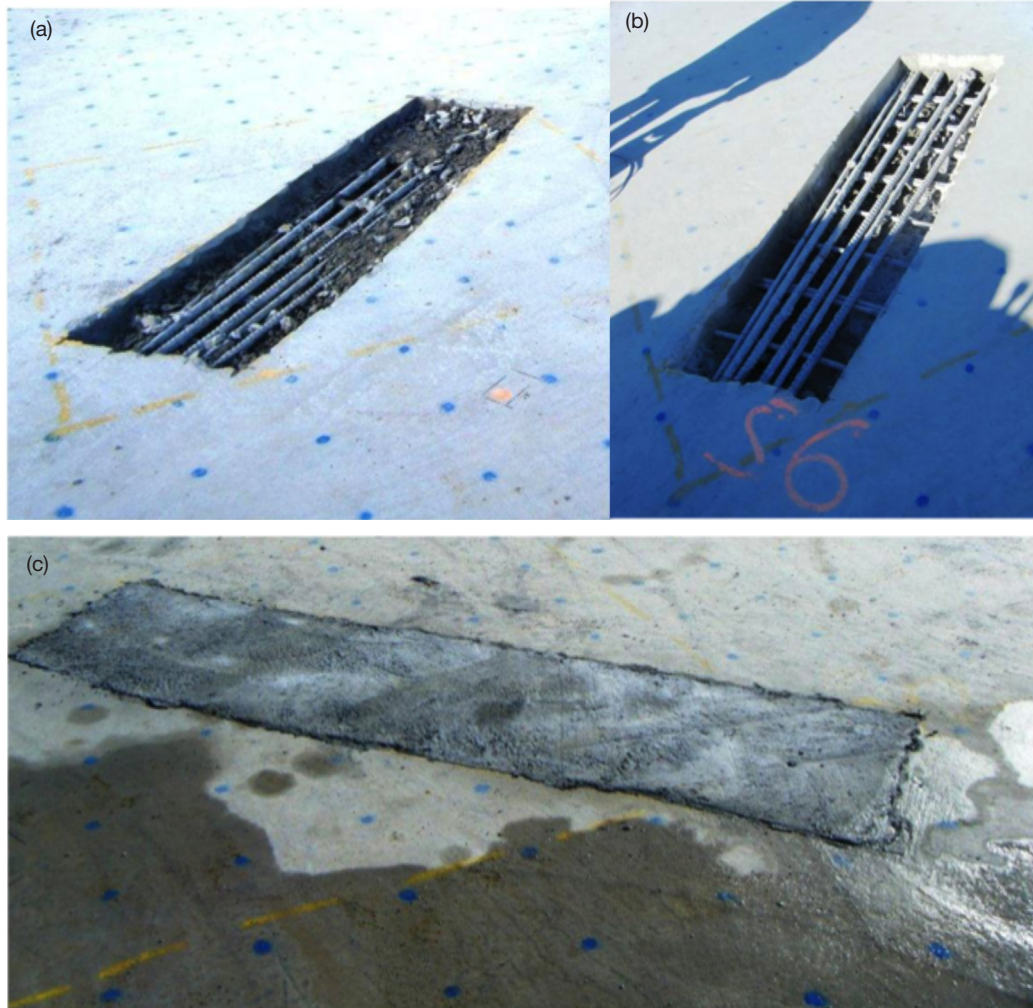


Figure 11. Remove and replace repair for an area with voiding. (a) Initial chipping of marked repair extents. (b) Chipping and inspections completed. (c) Repair concrete cast into prepared cavity.



Figure 12. Epoxy injection repairs at construction joint. (a) Areas of poor bond between placements at construction joint. (b) Epoxy injection of construction joint.